ACS APPLIED MATERIALS & INTERFACES

Research Article

www.acsami.org

Ultrafast Self-Healing of Polymer toward Strength Restoration

Xiao Ji Ye,[†] Ji-Long Zhang,[‡] Yong Zhu,[†] Min Zhi Rong,*[,†] Ming Qiu Zhang,*[,†] Yi Xi Song,[†] and Hong-Xing Zhang[‡]

[†]Key Laboratory for Polymeric Composite and Functional Materials of Ministry of Education, GD HPPC Lab, School of Chemistry and Chemical Engineering, Sun Yat-Sen University, Guangzhou 510275, P. R. China

[‡]State Key Laboratory of Theoretical and Computational Chemistry, Institute of Theoretical Chemistry, Jilin University, Changchun 130021, P. R. China

Supporting Information

ABSTRACT: Self-healing materials should take effect immediately following crack generation in principle, but the speed of autonomic recovery of mechanical properties through either extrinsic or intrinsic healing strategy reported so far is not that fast. Mostly, a couple of hours are taken for reaching steady state or maximum healing. To accelerate the healing process, the authors of this work make use of antimony pentafluoride as instant hardener of epoxy and successfully encapsulate the highly active antimony pentafluoride−ethanol complex in terms of hollow silica spheres. Accordingly, self-healing agent based on microencapsulated antimony pentafluoride−ethanol complex and epoxy monomer is developed. Epoxy material with the embedded healant capsules can thus be healed within a few seconds, as demonstrated by impact and fatigue tests. It is believed that the outcome presented here might help to move the self-healing technique closer to practical application, especially when the engineering significance of epoxy material is concerned.

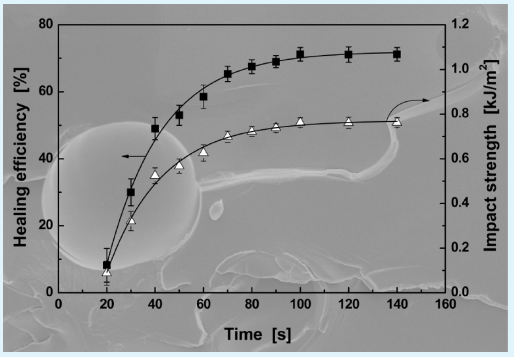

KEYWORDS: *self-healing, healing speed, Lewis acid, fast cure, epoxy*

1. INTRODUCTION

Self-healing polymeric materials have attracted more and more research interests.[1,2] Efforts are being made to develop extrinsic and intrinsic strategies for rebonding cracks, but the research concern mostly lies in the extent of mechanical properties restoration rather than the speed.[3−5] In fact, crack propagates very quickly (approximately at the velocity of sound or higher in rigid materials).[6,7] The materials should start to heal immediately following crack generation. Establishment of instant self-healing technique is necessary to avoid catastrophic failure in practical application, especially for the components in operation (like wings of flying aircrafts or pipelines conveying fluids). So far, the speed of autonomic recovery of mechanical properties is not that fast as revealed by the characteristic healing times documented in the literature (Table 1). In the best case, for example, the time taken for reaching steady state or maximum healing is on the level of hour or dozens of minutes.

By reviewing the existing self-healing methods,[1−5,8−23] we know that a fast healing would be achieved only when both thermodynamic and kinetic conditions are satisfied. From a thermodynamic point of view, strong chemical and/or physical interactions across the cracked planes should be established within a very short time, which is the necessary condition. Nevertheless, occurrence of such interactions has to be accompanied by fast contact between the interaction sites across the cracked planes, which is the sufficient condition from the angle of kinetics. For intrinsic self-healing driven by reversible bonding/debonding of macromolecules, chain mobility could not be high enough by nature to satisfy the above sufficient condition, not only in the case of stiff polymers but also in the case of elastomers. As a result, high speed intrinsic self-healing would be hard to be realized no matter how fast the healing chemistry is. In contrast, extrinsic self-healing might offer a solution, as the damage induced cracking of healing capsules leads to burst of the fluidic healant, which quickly delivers the healant to the places needed to be repaired. The key is to work out a fast healing chemistry capable of being integrated into polymers.

Our previous work showed that $BF_3{\cdot}O(C_2H_5)_2$−epoxy pair[10] allowed for quicker healing of cured epoxy compared with thiol−epoxy[9] (Table 1). Considering that (i) BF_3 belongs to Lewis acid, (ii) epoxy can also be cured by other Lewis acids like $TiCl_4$ and $AlCl_3$ via cationic polymerization,[24,25] and (iii) curing speed of epoxy catalyzed by Lewis acids is proportional to their acidity, we decided to formulate a fast healing system consisting of SbF_5 and epoxy. SbF_5 is a high performance fluidizer and has been employed in the pharmaceutical industry. It is the strongest Lewis acid except $AuF_5{\cdot}F_2$ [26] and able to react with almost all of the known chemical compounds. It is

Received: December 26, 2013
Accepted: February 12, 2014
Published: February 12, 2014

   dx.doi.org/10.1021/am405989b | ACS Appl. Mater. Interfaces 2014, 6, 3661−3670

Table 1. Healing Times of Selected Self-Healing Polymers for Mechanical Properties Restoration

material to be healed	healing system	healing mechanism	characteristic healing time[a]			assessment of healing effect	ref
			t_1	t_2	t_3		
epoxy vinyl esters	embedded exo-dicyclopentadiene- and Grubbs' catalyst-loaded capsules	ring-opening metathesis polymerization	2.5 min	5 min	48 h	tapered double cantilever beam (TDCB)	8
epoxy	embedded epoxy- and mercaptan/amine-loaded capsules	addition polymerization	15 min	1 h	24 h	TDCB	9
epoxy	embedded epoxy-loaded capsules and dispersed $BF_3{\cdot}O(C_2H_5)_2$	cationic polymerization	10 min	15−20 min	3 h	impact test	10
polyurethane	coumarin as photosensitive crosslinker	reversible photodimerization and cleavage		35 min	95 min	tensile test	11
polyurethane	alkoxyamines as thermally reversible crosslinker	reversible C−ON bond fission/ radical recombination	30 min	1 h	2 h	tensile test	12
hydrogen-bonded elastomer	graphene oxide as thermally reversible macrocrosslinker	reversible hydrogen bonding	1 min		1 h	tensile test	13
elastomer	supramolecular assembly	reversible hydrogen bonding	15 min	1−2 h	3 h	tensile test	14
co-polymer with polystyrene backbone and polyacrylate amide brushes	supramolecular crosslinking	reversible hydrogen bonding	15 min	1 h	24 h	tensile test	15
epoxy	embedded epoxy- and $SbF_5{\cdot}HOC_2H_5/HOC_2H_5$-loaded capsules	cationic polymerization	20 s	30−40 s	100 s	impact test	this work
epoxy	embedded epoxy- and $SbF_5{\cdot}HOC_2H_5/HOC_2H_5$-loaded capsules	cationic polymerization	15 s		20 s	fatigue test	this work

[a]Because no universally accepted criterion of healing speed is available, the authors define three characteristic healing times as follows to give an overall measure. t_1 = the time when measurable healing was firstly observed; t_2 = the time when healing efficiency reached 50% of the maximum value; t_3 = the time when healing efficiency reached steady state or the maximum value.

dx.doi.org/10.1021/am405989b | ACS Appl. Mater. Interfaces 2014, 6, 3661−3670

reasonable to expect that SbF_5 would not only serve as a low temperature hardener of epoxy following the same reaction mechanism as that involved in BF_3–epoxy cure, i.e., cationic polymerization, but also offer much faster curing speed owing to its extremely high activity. The objective of this work lies in verification of its role in accelerating self-healing.

2. EXPERIMENTAL SECTION

2.1. Materials. Epoxy, diglycidyl ether of bisphenol A (trade name EPON 828), was purchased from Shell Co., acting as both the composite's matrix and the polymerizable component of healing agent. Ethanol, tetraethyl orthosilicate (TEOS), polyvinylpyrrolidone (PVP), styrene, and methyl acrylate were all supplied by Alfa Aesar GmbH, Germany. Prior to use, styrene and methyl acrylate were washed with sodium hydroxide aqueous solution (5 wt %), thereafter three times with water, and dried over magnesium sulphate. Azobisisobutyronitrile (AIBN) was obtained from Sigma-Aldrich and purified by recrystallization. Ammonia (38 wt %) was purchased from Guangzhou Chemical Reagent Factory, China. SbF_5 was purchased from Tianjin Institute of Physical and Chemical Engineering of Nuclear Industry, China. Melamine and formaldehyde were provided by Shanghai Medical Group Reagent Co., China. Methyl hexahydrophthalic anhydride (MHHPA) and boron trifluoride–2,4-dimethylaniline complex (BF_3·DMA) were supplied by Energy Chemical, Shanghai, China.

2.2. Synthesis of Ethanol Solution of Antimony Pentafluoride–Ethanol Complex (SbF_5·HOC_2H_5/HOC_2H_5). Both absolute ethanol and ice bag were cool to −80 °C in advance. In the glove box filled with pure nitrogen gas, the ethanol (20 g) was poured into a polytetrafluoroethylene bottle in the ice bag, and then SbF_5 (5 g) was slowly added under stirring. The solution temperature was kept below 5 °C by controlling the dropping. Afterward, the solution was continuously stirred until it was warmed to room temperature, offering SbF_5·HOC_2H_5/HOC_2H_5, in which the fraction of SbF_5 is 20 wt %.

2.3. Preparation of Silica Walled Microcapsules Containing SbF_5·HOC_2H_5/HOC_2H_5. First, monodisperse poly(styrene methacrylate) (PSMA) particles (Figure S1) were prepared by dispersion polymerization. Deionized water (28 g), ethanol (140 g), and PVP (3 g) were stirred at a rate of 200 rpm in a 500 mL three-necked flask for 60 min at 75 °C under argon purge. Afterward, the solution of AIBN (2.3 g), styrene (74 g), and methyl acrylate (6 g) was added into the flask. After 12 h, the resultant PSMA particles were centrifuged, washed three times with water, and dried at 40 °C.

Then the precursor TEOS was coated onto the polymer microspheres by sol–gel process as follows. PSMA particles (5 g) were dispersed into ethanol (70 g) under ultrasonication. Deionized water (10 g), ammonia (4 mL), and TEOS (10 g) were incorporated to the system, respectively. The mixture was kept at ambient temperature for 24 h and then filtered to obtain silica coated particles. After removal of the PSMA template through high temperature calcination at 600 °C, hollow silica microcapsules (~6 μm) were obtained (Figure 1).

With the aid of vacuum,[27] SbF_5·HOC_2H_5/HOC_2H_5 was infiltrated into the hollow silica capsules to produce hardener-loaded capsules. Typically, hollow silica capsules (0.3 g) were submerged by the above SbF_5·HOC_2H_5/HOC_2H_5 in a 25 mL one-necked flask. Having been sealed and cooled to −20 °C, the system was evacuated to a vacuum degree of 0.001–0.002 mbar. After 50 h, the infiltration reached equilibrium, and the obtained SbF_5·HOC_2H_5/HOC_2H_5-loaded capsules (core content of 39 wt %) were filtered and purged with ethanol. The reason that SbF_5·HOC_2H_5/HOC_2H_5 was not encapsulated through in situ polymerization of melamine–formaldehyde in an oil-in-water emulsion[9] like the epoxy counterpart lies in the fact that the former is quite active and would be easily deactivated in water and common organic solvents except ethanol.

To know whether the activity of SbF_5·HOC_2H_5/HOC_2H_5 was changed after encapsulation, epoxy monomer (1 g) and SbF_5·HOC_2H_5/HOC_2H_5-loaded microcapsules (0.05 g) were mixed and ground. In the meantime, the drastic increase of temperature of the system due to rapid exotherm of curing was measured by infrared camera ImageIR 8300 (InfraTec GmbH, Germany). For comparison, SbF_5·HOC_2H_5/HOC_2H_5 (15 μL) was directly injected to epoxy monomer under stirring. The time dependence of temperature of the mixture was also recorded. The two curves resemble each other,

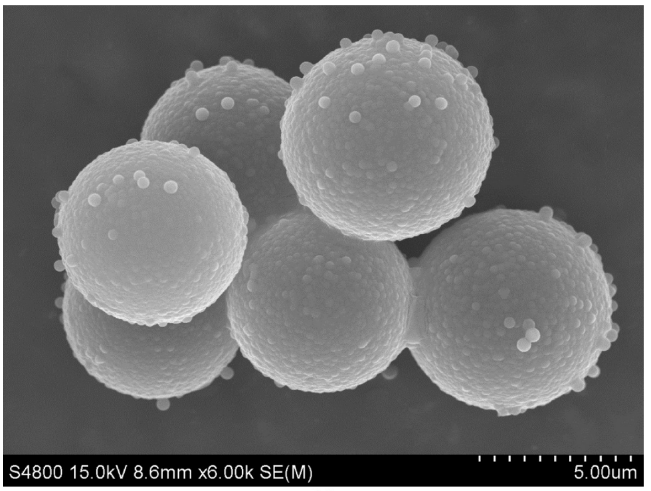

(a)

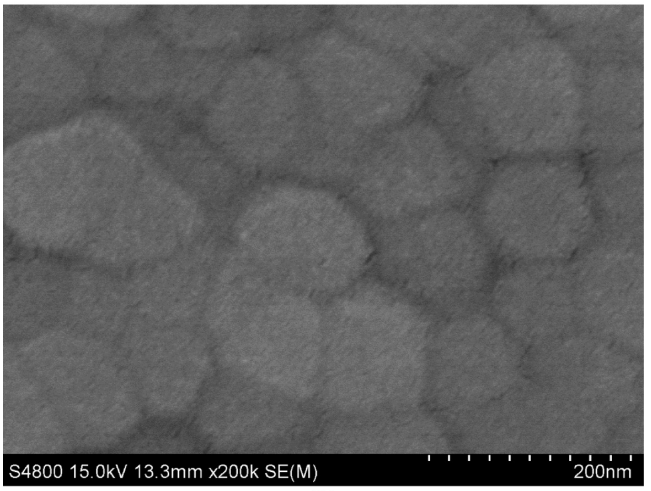

(b)

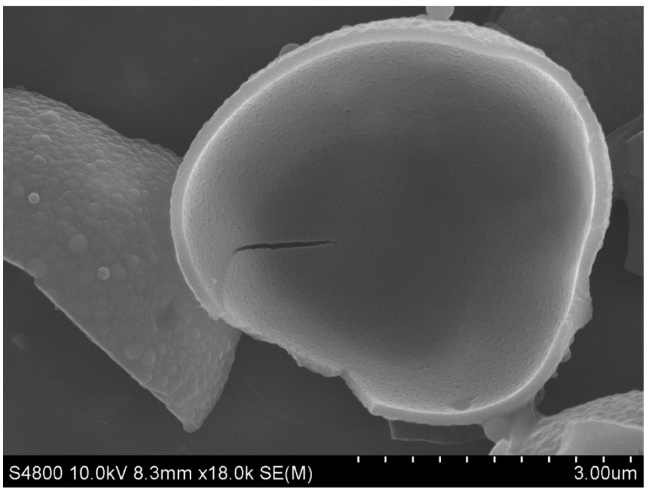

(c)

Figure 1. (a) Micrograph of hollow silica walled microcapsules, (b) high magnification view of the capsule surface, and (c) squashed capsules (showing thickness of the shell wall is about 200 nm).

dx.doi.org/10.1021/am405989b | ACS Appl. Mater. Interfaces 2014, 6, 3661–3670

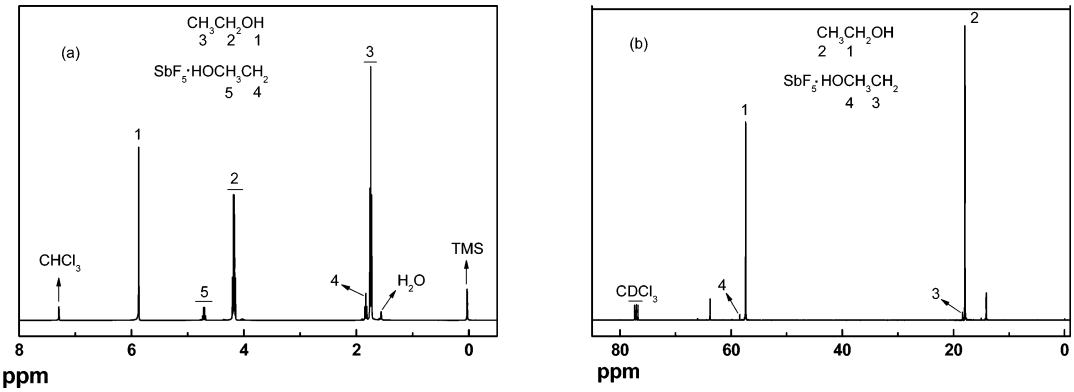

Figure 2. (a) ^{1}H NMR and (b) ^{13}C NMR spectra of ethanol solution of antimony pentafluoride−ethanol complex (with molecular ratio of SbF_5/HOC_2H_5 = 0.002 at 25 °C).

meaning that the encapsulated SbF_5·HOC_2H_5/HOC_2H_5 maintains its reactivity of curing epoxy (Figure S2).

Core content of the SbF_5·HOC_2H_5/HOC_2H_5-loaded microcapsules was determined by the following procedures. First, a certain amount of capsules were mixed with some ethanol, which were then completely ground in an agate mortar to release the encapsulated SbF_5·HOC_2H_5/HOC_2H_5. The mixture was filtered and washed three times with ethanol to isolate the shell. The remaining liquid was added to the mixture of thick HNO_3 and H_2SO_4 ($^1/_5$ by volume) and treated in a 750 W microwave oven for 2 min to dispel the organic matter. After 24 h, the solution was examined by a TJA IRIS (HR) inductively coupled plasma atomic emission spectrometer to determine the concentration of Sb, β. The core content, γ, was calculated from $\gamma = \Gamma\beta M_{SbF_5}/(0.2\alpha M_{Sb})$, where α is the capsule's weight, Γ is the volume of the acid solution containing the separated SbF_5·HOC_2H_5/HOC_2H_5, and M_{SbF_5} and M_{Sb} are the molecular weights of SbF_5 and Sb, respectively.

2.4. Preparation of Epoxy-Loaded Microcapsules and Self-Healing Epoxy Composite. Epoxy monomer was encapsulated by poly(melamine formaldehyde) (PMF) (Figure S3) as mentioned in ref 9. The average diameter and core content of the resultant epoxy-loaded capsules (determined by extraction method[9]) are 130 μm and 91 wt %, respectively. Unfilled epoxy specimens were cast from a mixture of 5 parts BF_3·DMA, 80 parts MHHPA, and 100 parts EPON 828, while the self-healing epoxy specimens were prepared by uniformly blending 10 wt % epoxy-loaded microcapsules and 0.6 wt % SbF_5·HOC_2H_5/HOC_2H_5-loaded microcapsules with the aforesaid mixture of BF_3·DMA, MHHPA, and EPON 828. The compounds were degassed, poured into a preheated closed silicone rubber mold, and cured at 50 °C for 60 h and 70 °C for 12 h. The control specimen has the same composition as the self-healing one except that the hardener capsules are replaced by ethanol capsules.

2.5. Characterization. ^{1}H nuclear magnetic resonance (NMR) and ^{13}C NMR spectra were collected by a Bruker Avance III spectrometer (400 MHz). Morphological observation was conducted on a HITACHI model S-4800 field emission scanning electron microscope (SEM).

To monitor the curing reaction in terms of exotherm, optical pyrometry[28] was used. Different dosages (1, 5, 10, and 15 μL) of SbF_5·HOC_2H_5/HOC_2H_5 (with SbF_5 concentration of 20 wt %) were injected to epoxy monomer (1 g) under stirring, respectively. Afterward, temperature change of the system was recorded by means of infrared camera ImageIR 8300 (InfraTec GmbH, Germany). Fourier transform infrared (FTIR) spectra were recorded by a Bruker EQUINOX55 spectrometer coupled to an infrared microscope spectrometer. Prior to the measurement, epoxy monomer was coated on a KBr plate. Then SbF_5·HOC_2H_5/HOC_2H_5 was sprayed onto the epoxy, and the test starts immediately. To shorten the test time, the scanning wave number range was set from 900 to 930 cm^{-1} so that only the absorption of epoxy groups was observed during curing.

Sizes of the microcapsules were determined by Malvern MasterSizer 2000 particle size analyzer.

Healing ability of the materials damaged by monotonic fracture was assessed by impact test.[29] The test was conducted at 25 °C on Izod notched specimen (52.8 × 12.3 × 10.1 mm^3) according to ASTM D265-034 using a JJ-20 impact tester produced by Changchun Research Institute for Testing Machines Co. Ltd., China. The specimen was impacted to failure, and then the crack faces were allowed to come back into contact as fast as possible. The specimen was healed at 25 °C under a gentle pressure of ∼0.2 MPa for a period of time. Finally, the healed specimen was impacted again. Healing efficiency is defined as the ratio of impact strength of healed and virgin materials. Each batch included five specimens to yield averaged values.

Healing of the materials under cyclic stress was evaluated by fatigue test on tapered double cantilever beam (TDCB) specimens (with groove length of 55 mm[30]) with a Shimadzu air servo fatigue and endurance testing system ADT-AV02K1S5 with 2 kN load cell at 25 °C. The specimens were precracked (∼2.5 mm long) by a razor blade while ensuring the precrack tip was centered in the groove. The specimen was cyclically loaded immediately after removal of the blade. A triangular waveform of 5 Hz was applied with a stress ratio, R, of 0.1 ($R = K_{min}/K_{max}$, where K_{min} and K_{max} denote the minimum and maximum values of the cyclic stress intensity, respectively). Fatigue cracks were grown within constant mode-I stress intensity factor range, ΔK_I ($\Delta K_I = K_{max} - K_{min}$). The optically measured crack tip position and specimen compliance were plotted against number of cycles. The linear relationship between optically measured crack length and specimen compliance was used to calculate the crack tip position of the specimens at all times during the experiment.[31] Healing efficiency, λ, was defined by fatigue life extension:[32] $\lambda = (N_{healed} - N_{control})/N_{control}$, where N_{healed} and $N_{control}$ denote the total number of cycles to failure of the healed specimen and that of a similar control specimen without healing, respectively. For each test, the result was an average of five specimens. Temperature variation at the crack tip was simultaneously examined by infrared camera ImageIR 8300 (InfraTec GmbH, Germany). Besides, fracture toughness, K_{IC}, of the unfilled and self-healing materials was also measured using TDCB specimens.

3. RESULTS AND DISCUSSION

SbF_5 alone has not yet directly served as curing agent of epoxy probably because of its outstanding reactivity, which makes it difficult to be handled and limits its effective usage. In this context, antimony pentafluoride−ethanol complex (SbF_5·$(HOC_2H_5)_n$) should be an effective alternative, as SbF_5 molecules are stabilized in the complex without losing its valuable catalytic activity. It is worth noting that antimony pentafluoride−ethanol complex has not yet been commercialized and no scientific papers concerning its structure and properties are available. We have to acquire some fundamental understanding of the chemical prior to application.

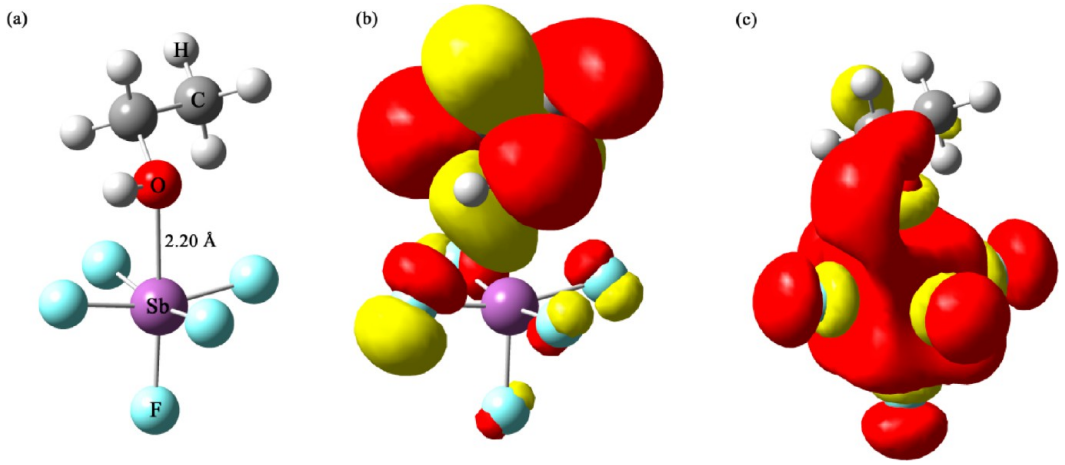

Figure 3. (a) Calculated molecular structure of SbF_5–ethanol complex (stoichiometric ratio of SbF_5 and ethanol is 1:1), (b) the highest occupied molecular orbital (HOMO) plot, and (c) the lowest unoccupied molecular orbital (LUMO) plot.

It is believed that donor–acceptor bonding[33] governs the interaction between SbF_5 and ethanol in the complex. The O atom in ethanol (acting as donor molecule) possesses an unshared pair of electrons in the valence shell, while the Sb in SbF_5 (acting as acceptor) has a suitable unoccupied orbital. Accordingly, lone pair electrons of oxygen atoms in ethanol tend to fill the empty orbits of antimony atoms, forming coordination bonds. As a result, electron cloud density of the methylene connected to the oxygen atom is decreased, as characterized by the shift of the CH_2-O peak (2) to low field peak (5) in the ^{1}H NMR spectrum (Figure 2a). Correspondingly, the mild shift of methyl proton peak 3 to peak 4 also reflects this transfer of electrons but is less evident because it is far away from oxygen atom. Similarly, in the ^{13}C NMR spectrum (Figure 2b), the shift of both methylene and methyl peaks to low field can also be observed. The results confirm the coordination complexation between ethanol and SbF_5.

To further determine the chemical composition of $SbF_5 \cdot (HOC_2H_5)_n$, quantum calculation is implemented with Gaussian software package (see Supporting Information for more details). As exhibited in Figure 3a, when stoichiometric ratio of SbF_5 and ethanol is 1:1, the O atom of ethanol coordinates with Sb atom, forming a six-coordinated complex (i.e., $SbF_5 \cdot HOC_2H_5$), regardless of on which surface of the triangular bipyramid configuration of SbF_5 the ethanol molecule sticks. The length of Sb–F bond in the complex is 1.84 Å, and that of Sb–O bond is 2.20 Å. Orbit analysis indicates that highest occupied molecular orbital (HOMO) of the six-coordinate structure is mainly concentrated on the ethanol ligand (Figure 3b), while lowest unoccupied molecular orbital (LUMO) is concentrated on Sb (Figure 3c).

In addition, quantum calculations are also carried out for other stoichiometric ratios of SbF_5 and ethanol (1:1.5, 1:2, 1:2.5, 1:3, 1:3.5, and 1:4). For the ratio of 1:1.5, 1:2, and 1:3, similar six-coordinated Sb is perceived (Figures S4, S5, and S6), in which the Sb–O bond length ranges from 2.13 to 2.16 Å. The orbit distributions of these coordination structures resemble the case of 1:1, implying that only one ethanol molecule and one SbF_5 molecule form the coordination complex (i.e., $SbF_5 \cdot HOC_2H_5$). However, no stable structure can be obtained when the ratios are 1:2.5 and 1:3.5. With respect to the ratio of 1:4, two ethanol molecules coordinate with one Sb atom (Figure S7). The Sb atom appears to be seven-coordinated, and bond lengths of Sb–F and Sb–O are 2.30 and 2.26 Å, respectively, which are too long to stabilize the complex structure. Therefore, six-coordinated Sb is the most reasonable, and the chemical composition of the complex can thus be considered as $SbF_5 \cdot HOC_2H_5$.

Since curing behavior of epoxy in the presence of $SbF_5 \cdot HOC_2H_5$ has not been revealed, optical pyrometry[28] and infrared microscopy are used. Conventional differential scanning calorimetry (DSC) is no longer applicable as polymerization considerably proceeds before homogeneous mixture of the components is obtained. The data of thermal imaging (Figure 4) show that soon after the ethanol solution of

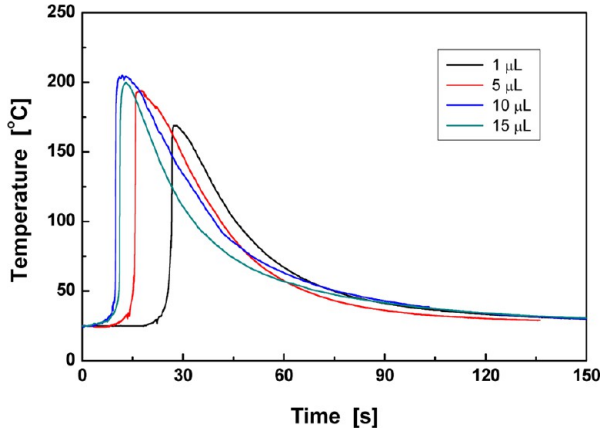

Figure 4. Time dependence of temperature of epoxy cured by ethanol solution of antimony pentafluoride–ethanol complex ($SbF_5 \cdot HOC_2H_5$/HOC_2H_5).

antimony pentafluoride–ethanol complex ($SbF_5 \cdot HOC_2H_5$/HOC_2H_5) is added to epoxy, rapid solidification occurs as characterized by the drastic increase of temperature from ambient temperature to the maximum (i.e., ~200 °C) within several seconds. When the dosage of $SbF_5 \cdot HOC_2H_5/HOC_2H_5$ increases from 1 to 10 μL, the time for reaching the maximum temperature is greatly shortened and the maximum temperature is obviously increased. When the hardener dosage is further raised from 10 to 15 μL, however, both the peak position and height are basically the same. The behavior follows the general rule of curing of epoxy in the presence of Lewis

dx.doi.org/10.1021/am405989b | ACS Appl. Mater. Interfaces 2014, 6, 3661–3670

acid. That is, once the dosage of Lewis acid reaches the prescribed minimum, cationic chain polymerization of epoxy begins. The curing reaction is nearly independent of Lewis acid content when the latter exceeds a certain value. Accordingly, Scheme 1 illustrates the reaction mechanism involved.

Scheme 1. Mechanism of the Reaction between SbF_5·HOC_2H_5 and Epoxy

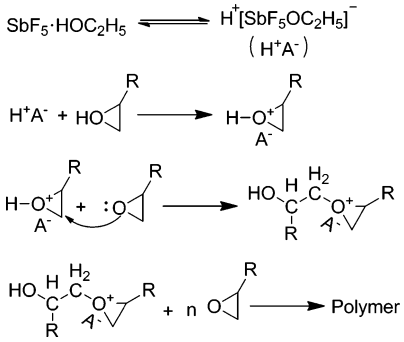

A more detailed kinetics study is given by the real-time microinfrared spectra (Figure 5), which shows that the amount of epoxide groups decreases with time. About 94% epoxide groups are consumed after 10 s when the chemicals are contacted. Because the spectra were continuously collected from the same site of the sample, the possible influence of sample thickness, heterogeneity, etc. can be neglected when calculating the curing degree based on the peak areas.

Now SbF_5·HOC_2H_5/HOC_2H_5 has proved to be able to initiate fast curing of epoxy, its capability for fast repairing cracks in polymer in cooperation with unreacted epoxy monomer is worth being verified by means of dual microcapsules approach.[1] Although SbF_5·HOC_2H_5 becomes less corrosive than SbF_5, it is still highly active and could not be encapsulated by conventional technique like emulsion polymerization. Accordingly, silica walled microcapsules containing SbF_5·HOC_2H_5/HOC_2H_5 were prepared and embedded in epoxy matrix together with epoxy capsules to build up self-healing epoxy composite.

On the basis of the protocol proposed by Jones et al.,[29] notched impact tests were carried out to evaluate healing effect of cured epoxy with embedded capsules, which contain epoxy monomer and SbF_5·HOC_2H_5/HOC_2H_5, respectively. Efficiency of healing is defined as the ratio of impact strengths of healed and virgin materials. As expected, the healing agent can be liberated upon fracture of the specimen, spreading over the fractured surface and rejoining the broken specimen at room temperature (Figure 6). In contrast, the impacted control specimen, which has the same composition as the self-healing specimen except that SbF_5·HOC_2H_5/HOC_2H_5 microcapsules are replaced by ethanol microcapsules, could not be rebonded. More importantly, the dependence of healing efficiency on healing time (Figure 7) shows that about 8.3% impact strength is recovered after 20 s and the maximum healing efficiency is acquired after 100 s of the healing time. The results demonstrate that the healing agent not only allows for autonomic healing of cured epoxy without manual intervention but also obviously accelerates the healing process owing to the translation of curing kinetics.

To understand whether the SbF_5 dispersed in the matrix would affect long term stability of the healed epoxy, we did the following experiments. First, the self-healing specimens were impacted to failure, and then the broken halves were reconnected for healing at room temperature. After 10 months, the healed specimens were tested by impact again. The average healing efficiency was 71.2 ± 1.5%, which equals the steady state healing efficiency of fresh made specimens (Figure 7). Clearly, SbF_5 does not exert detectable influence on the stability of healed epoxy. The result is understandable because the hardener SbF_5·HOC_2H_5 is milder than SbF_5 and even inert to air. Moreover, the content of SbF_5 dispersed in the self-healing composite is low because of the low concentration of the hardener capsules (i.e., 0.6 wt %).

Nevertheless, it is worth noting that curing of SbF_5–epoxy system is approximately completed within 10 s as revealed by infrared spectroscopy (Figure 5), which is roughly equivalent to the time for collecting the impact broken specimen and reassembling for crack healing (8–10 s). It means that a certain degree of polymerization must have taken place prior to the occurrence of healing reaction across the broken surfaces (i.e. contact of the broken surfaces), despite that the fluidic healing chemicals from the ruptured capsules need time to flow out and meet each other for the subsequent reaction. In fact, healing of cracks is multiconvoluted time dependent.[34] With regard to the present fast curing system, the data of impact tests (Figure 7) only give a rough description of the healing kinetics. For purposes of more exactly identifying (initial) healing time or healing speed, the time taken for recombination of broken

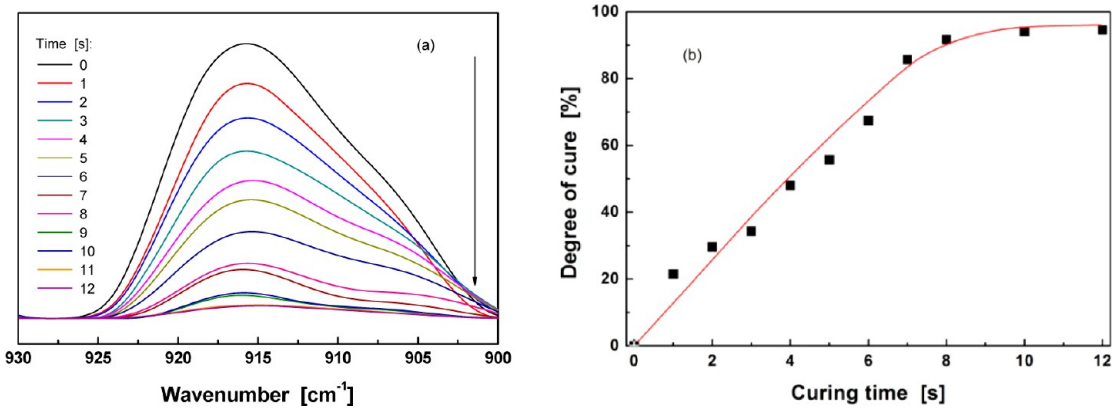

Figure 5. (a) Infrared absorption of epoxide groups as a function of time when epoxy meets SbF_5·HOC_2H_5/HOC_2H_5 (20 wt %). (b) Evolution of curing degree of epoxy calculated with the peak areas in (a).

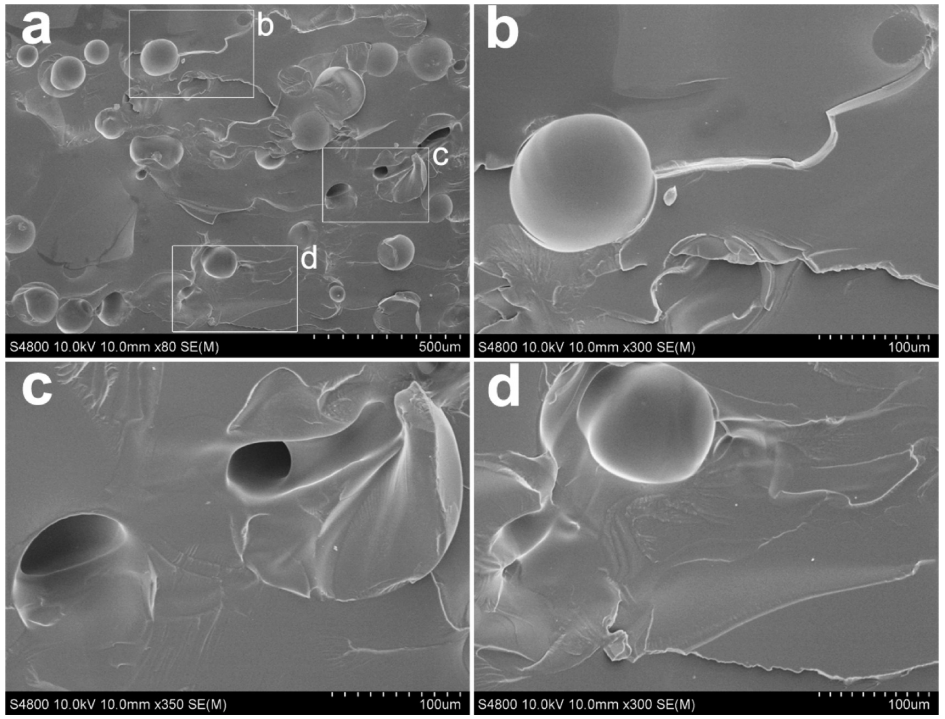

Figure 6. (a) SEM image of impact fracture surface of healed self-healing specimen. The specimen had been fractured by the first impact test, healed at 25 °C for 100 s, and then fractured again by the second impact test. (b–d) Magnified views of different parts of (a).

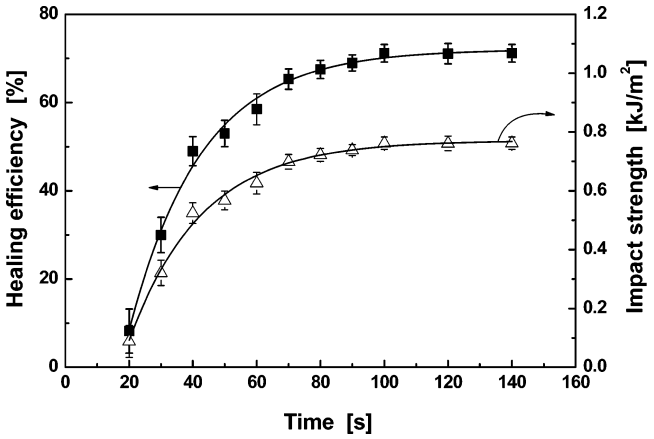

Figure 7. Healing efficiency versus healing time of self-healing specimens determined by impact test. Impact strength of the virgin self-healing specimen is 1.070 ± 0.025 kJ/m^2.

specimens before healing should be shortened to the greatest extent.

By screening the available destructive testing methods including tensile, tearing, etc., we found that fatigue measurement seems to be the most appropriate to fulfill the task as the cracked planes are rapidly opened and closed under cyclic stress without the necessity of "time consuming" manual reassembling. The frequent opening and closing also promote transportation and mixing of the healing fluids out of the broken capsules. Meanwhile, the time dependent self-healability of fatigue crack offered by the healing agent can be determined.

To minimize the influence of curing reaction of the healing agent released from the broken capsules after precracking but prior to fatigue test, the time for precracking and attaching the specimen to the fixing jig of fatigue tester was managed to be as short as possible (5–7 s). Moreover, removal of the razor blade for making precrack was synchronized to the start of fatigue test. It is found that when the blade is removed after making the precrack, a large portion of the precracked faces is allowed to touch each other (Figure S8). On the contrary, the two faces are mostly separated so long as the blade stays put. Therefore, for the precracked self-healing specimen containing microencapsulated healing agent without removal of the blade, polymerization of the released healing agent would be greatly hindered in the interface region. In case fatigue test starts immediately after removal of the blade, the healing time can be roughly reckoned from the start of fatigue test, supposing that the healing reaction across the crack faces mainly occurs after beginning of the fatigue test.

Figure 8a plots crack length against fatigue cycle of unfilled epoxy, control, and self-healing specimens. Because effects of (i) microcapsules induced toughening (Figure S9), (ii) hydrodynamic pressure crack tip shielding, (iii) polymeric wedge made of cured healing agent, and (iv) adhesive bonding of the healing agent (Figure S10) are responsible for the extension of fatigue life of self-healing polymer with encapsulated healant,[31,32,35,36] the control specimen was prepared according to the same formulation like the self-healing one except that the hardener capsules are replaced by ethanol capsules to highlight factors iii and iv of the self-healing specimen. Compared to both unfilled epoxy and control specimens, the self-healing specimen exhibits remarkably reduced crack growth rate (Figure 8a). The latter two mechanisms of the healing agent mentioned above play the leading role. The room temperature healing efficiency defined by fatigue life extension[32] is estimated to be 167% relative to the control specimen and 304% to the unfilled epoxy specimen. Furthermore, the healability remains unchanged within 8 months (Figure 9).

More detailed information about the fatigue retardation behavior of the healing agent can be found in the load–

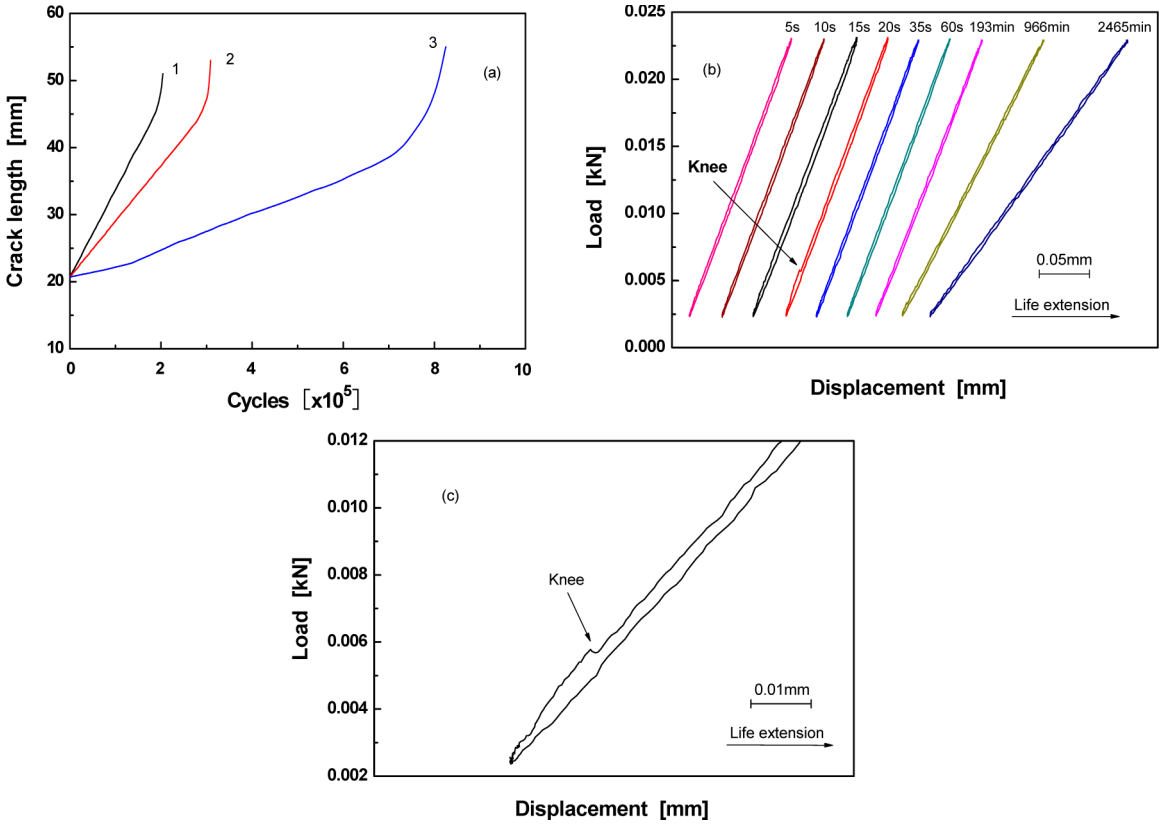

Figure 8. (a) Crack length versus fatigue cycle of (1) neat epoxy, (2) control, and (3) self-healing specimens. (b) Load−displacement curves of self-healing specimen measured during selected cycles in (a). The times counted from starting of the fatigue test are shown on top of the corresponding curves. (c) Enlarged view of the curve of 20 s in (b) showing the knee phenomenon. Testing conditions were the following: K_{max} = 0.258 MPa $m^{1/2}$, K_{min} = 0.026 MPa $m^{1/2}$, ΔK_I = 0.232 MPa $m^{1/2}$.

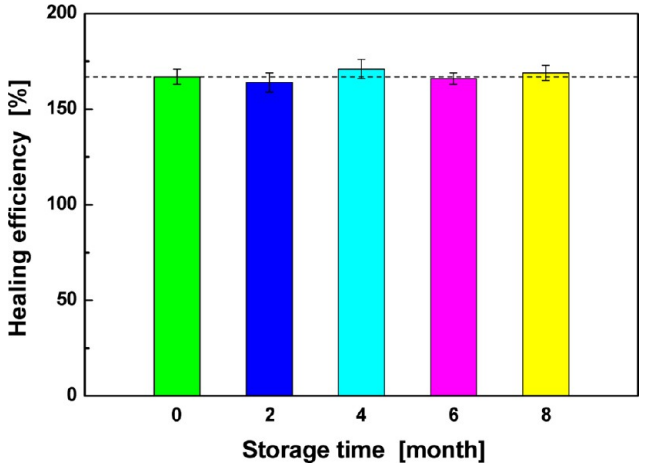

Figure 9. Effect of storage time in ambient air on healing efficiency of the self-healing specimens determined by fatigue test. Testing conditions were the following: K_{max} = 0.258 MPa $m^{1/2}$; K_{min} = 0.026 MPa $m^{1/2}$; ΔK_I = 0.232 MPa $m^{1/2}$.

displacement curves (Figure 8b and Figure 8c). The viscous flow of the released healing agent on the crack plane results in the appearance of hysteresis at the beginning of the test. With a rise in time, the hysteresis loop area increases and then decreases to constant. It implies that the healing agent liberated by precracking starts to be polymerized, enhancing the hydrodynamic pressure effect ascribed to the increased viscosity. Afterward, this effect is reduced because of (i) further polymerization (hardening) of the healing agent released during precracking and (ii) less amount of fluidic healing agent refilled by the gradually broken capsules on the crack growth path compared to that offered in one go by the precracked portion (~2.5 mm long). In this context, it is known that the first mechanically detectable gel (healing) time is 15 s (refer to the loop of 15 s in Figure 8b showing the largest area).

In addition, a knee point is observed on the loading part of the loop of 20 s (Figure 8b and Figure 8c), representing crack closure effect contributed by the polymeric wedge and adhesion at the crack tip.[37] Such a phenomenon is absent in the case of control specimen, in which the released epoxy monomer cannot be crosslinked because of the lack of hardener. Since the results in Figure 8a reveal that (i) the mechanisms of polymeric wedge and adhesive bonding, rather than microcapsules induced toughening and hydrodynamic pressure, predominate crack retardation and (ii) crack grows steadily prior to failure, the time when the knee point is perceived (i.e., 20 s, refer to Figure 8c) can be regarded as the time when the healing effect reaches the maximum under cyclic loading. That is, the solidified healing agent provides the largest closure effect at the knee point. Subsequently, the crack grows past the wedge from the cured healing agent due to higher ΔK_I. Although the above data are acquired within the precrack region, which might generate experimental errors of fatigue performance measurement due to slight deflection of the precrack, the rapid healability has been fully demonstrated.

The analysis is supported by the in situ temperature measurement of the crack tip of the self-healing specimen during fatigue test (Figure 10). With an increase of the test

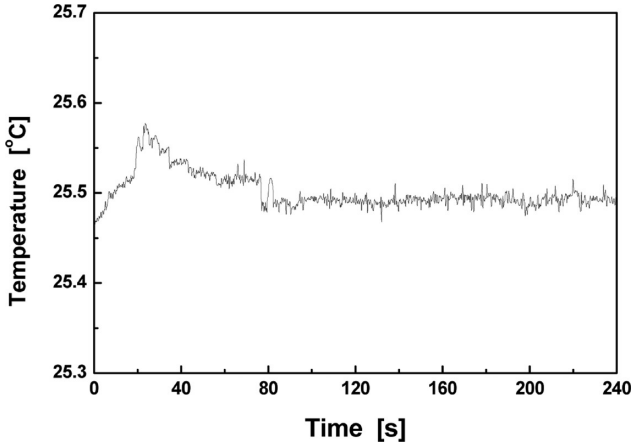

Figure 10. Temperature of crack tip of self-healing specimen as a function of time recorded by infrared camera during fatigue test. The time is counted from starting of the fatigue test.

time, the temperature at the crack tip region increases and then keeps at a slightly lower level. It coincides with the aforesaid rapid exotherm of epoxy cured by $SbF_5{\cdot}HOC_2H_5/HOC_2H_5$ (Figure 4 and Figure 5). That is, because the released healing agent in the pre-crack tip is polymerized, the reaction temperature peaks up within very short time accordingly. When the precrack does not obviously move forward, no additional healing agent can be refilled so that the on-site temperature decreases within the time range of interest. Here, the highest reaction temperature is found at ~20 s, in agreement with the time of presence of knee point on the load−displacement curve (Figure 8b).

4. CONCLUSIONS

The self-healing system based on SbF_5−epoxy pair combines fast healing chemistry and highly mobile healing fluid so that the time required to realize room temperature healing is shortened to seconds (Table 1). Although the determination of healing times might be not precise enough because of the testing methods, the results of impact and fatigue tests are mutually corroborated, confirming the ultrafast healability of the material.

It is believed that the significantly improved self-healing speed would help to move the smart functionality closer to practical application. The drastic exotherm produced by the curing (healing) reaction (Figure 4) would be particularly useful for operation in cold environment (like the sky) or winter. Since epoxy has been widely used as structural material in industry, a variety of products based on epoxy (including aerospace, automotive, and electronic composites) would benefit from this performance. Moreover, by taking advantage of easy processability of encapsulated healant and strong adhesiveness of epoxy, the present healing system might be transferred to other polymers for quickly recovering load-bearing ability.

■ ASSOCIATED CONTENT

Supporting Information

SEM photos of PSMA particles and epoxy capsules, time dependence of temperature of epoxy cured by $SbF_5{\cdot}HOC_2H_5/HOC_2H_5$, quantum calculations for the complex, groove of precracked TDCB specimen, K_{IC} of self-healing specimens, and SEM photos of fatigue fracture surface. This material is available free of charge via the Internet at http://pubs.acs.org.

■ AUTHOR INFORMATION

Corresponding Authors

*M.Z.R.: phone, +86-20-84114008; fax, +86-20-84114008; e-mail, cesrmz@mail.sysu.edu.cn.

*M.Q.Z.: phone, +86-20-84114008; fax, +86-20-84114008; e-mail, ceszmq@mail.sysu.edu.cn.

Notes

The authors declare no competing financial interest.

■ ACKNOWLEDGMENTS

The authors thank the support of the Natural Science Foundation of China (Grants 51273214, 20874117, 51073176, and 51333008), Doctoral Fund of Ministry of Education of China (Grant 20090171110026), the Science and Technology Program of Guangdong Province (Grants 2010B010800021, 2010A011300004, 2011A091102001, and S2013020013029), and the Basic Scientific Research Foundation in Colleges and Universities of Ministry of Education of China (Grant 12lgjc08).

■ REFERENCES

(1) Zhang, M. Q.; Rong, M. Z. *Self-Healing Polymers and Polymer Composites*; John Wiley & Sons: Hoboken, NJ, 2011.

(2) Binder, W. H. *Self-Healing Polymers*; Wiley-VCH: Weinheim, Germany, 2013.

(3) Billiet, S.; Hillewaere, X. K.; Teixeira, R. F.; Du Prez, F. E. Chemistry of Crosslinking Processes for Self-Healing Polymers. *Macromol. Rapid Commun.* **2013**, *34*, 290−309.

(4) Zhang, M. Q.; Rong, M. Z. Intrinsic Self-Healing of Covalent Polymers through Bond Reconnection towards Strength Restoration. *Polym. Chem.* **2013**, *4*, 4878−4884.

(5) Zhang, M. Q.; Rong, M. Z. Self-Healing Polymeric Materials towards Strength Recovery for Structural Application. *Acta Polym. Sin.* **2012**, *11*, 1183−1199.

(6) Rosakis, A. J.; Samudrala, O.; Singh, R. P.; Shukla, A. Intersonic Crack Propagation in Bimaterial Systems. *J. Mech. Phys. Solids* **1998**, *46*, 1789−1814.

(7) Broberg, K. B. The Near-Tip Field at High Crack Velocities. *Int. J. Fract.* **1989**, *39*, 1−13.

(8) Wilson, G. O.; Moore, J. S.; White, S. R.; Sottos, N. R.; Andersson, H. M. Autonomic Healing of Epoxy Vinyl Esters via Ring Opening Metathesis Polymerization. *Adv. Funct. Mater.* **2008**, *18*, 44−52.

(9) Yuan, Y. C.; Rong, M. Z.; Zhang, M. Q.; Chen, J.; Yang, G. C.; Li, X. M. Self-Healing Polymeric Materials Using Epoxy/Mercaptan as the Healant. *Macromolecules* **2008**, *41*, 5197−5202.

(10) Xiao, D. S.; Yuan, Y. C.; Rong, M. Z.; Zhang, M. Q. A Facile Strategy for Preparing Self-Healing Polymer Composites by Incorporation of Cationic Catalyst-Loaded Vegetable Fibers. *Adv. Funct. Mater.* **2009**, *19*, 2289−2296.

(11) Ling, J.; Rong, M. Z.; Zhang, M. Q. Photo-Stimulated Self-Healing Polyurethane Containing Dihydroxyl Coumarin Derivatives. *Polymer* **2012**, *53*, 2691−2698.

(12) Yuan, C. E.; Rong, M. Z.; Zhang, M. Q. *Polymer* (DOI: 10.1016/j.polymer.2014.02.033).

(13) Wang, C.; Liu, N.; Allen, R.; Tok, J. B. H.; Wu, Y.; Zhang, F.; Chen, Y.; Bao, Z. A Rapid and Efficient Self-Healing Thermo-Reversible Elastomer Crosslinked with Graphene Oxide. *Adv. Mater.* **2013**, *25*, 5785−5790.
(14) Cordier, P.; Tournilhac, F.; Soulié-Ziakovic, C.; Leibler, L. Self-Healing and Thermoreversible Rubber from Supramolecular Assembly. *Nature* **2008**, *451*, 977−980.
(15) Chen, Y.; Kushner, A. M.; Williams, G. A.; Guan, Z. Multiphase Design of Autonomic Self-Healing Thermoplastic Elastomers. *Nat. Chem.* **2012**, *4*, 467−472.
(16) Blaiszik, B. J.; Kramer, S. L. B.; Olugebefola, S. C.; Moore, J. S.; Sottos, N. R.; White, S. R. Self-Healing Polymers and Composites. *Annu. Rev. Mater. Res.* **2010**, *40*, 179−211.
(17) White, S. R.; Sottos, N. R.; Geubelle, P. H.; Moore, J. S.; Kessler, M. R.; Sriram, S. R.; Brown, E. N.; Viswanathan, S. Autonomic Healing of Polymer Composites. *Nature* **2001**, *409*, 794−797.
(18) Toohey, K. S.; Sottos, N. R.; Lewis, J. A.; Moore, J. S.; White, S. R. Self-Healing Materials with Microvascular Networks. *Nat. Mater.* **2007**, *6*, 581−585.
(19) Kamphaus, J. M.; Rule, J. D.; Moore, J. S.; Sottos, N. R.; White, S. R. A New Self-Healing Epoxy with Tungsten (VI) Chloride Catalyst. *J. R. Soc., Interface* **2008**, *5*, 95−103.
(20) Blaiszik, B. J.; Caruso, M. M.; McIlroy, D. A.; Moore, J. S.; White, S. R.; Sottos, N. R. Microcapsules Filled with Reactive Solutions for Self-Healing Materials. *Polymer* **2009**, *50*, 990−997.
(21) Wilson, G. O.; Caruso, M. M.; Reimer, N. T.; White, S. R.; Sottos, N. R.; Moore, J. S. Evaluation of Ruthenium Catalysts for Ring-Opening Metathesis Polymerization-Based Self-Healing Applications. *Chem. Mater.* **2008**, *20*, 3288−3297.
(22) Wilson, G. O.; Henderson, J. W.; Caruso, M. M.; Blaiszik, B. J.; McIntire, P. J.; Sottos, N. R.; White, S. R.; Moore, J. S. Evaluation of Peroxide Initiators for Radical Polymerization-Based Self-Healing Applications. *J. Polym. Sci., Part A: Polym. Chem.* **2010**, *48*, 2698−2708.
(23) Mauldin, T. C.; Rule, J. D.; Sottos, N. R.; White, S. R.; Moore, J. S. Self-Healing Kinetics and the Stereoisomers of Dicyclopentadiene. *J. R. Soc., Interface* **2007**, *4*, 389−393.
(24) Pencezek, S.; Kubisa, P.; Matyjaszewski, K. *Cationic Ring-Opening Polymerization Part II: Synthetic Applications*; Springer: Berlin, 1985.
(25) Matyjaszewski, K. *Cationic Polymerization: Mechanisms, Synthesis, and Applications*; Marcel Dekker: New York, 1996.
(26) Olah, G. A.; Prakash, G. K. S.; Wang, Q.; Li, X. Y. In *Encyclopedia of Reagents for Organic Synthesis*; Paquette, L., Ed.; John Wiley & Sons: New York, 1995; pp 2715−2716.
(27) Xiao, D. S.; Yuan, Y. C.; Rong, M. Z.; Zhang, M. Q. Hollow Polymeric Microcapsules: Preparation, Characterization and Application in Holding Boron Trifluoride Diethyl Etherate. *Polymer* **2009**, *50*, 560−568.
(28) Crivello, J. V. Redox Initiated Cationic Polymerization: Reduction of Diaryliodonium Salts by 9-BBN. *J. Polym. Sci., Part A: Polym. Chem.* **2009**, *47*, 5639−5651.
(29) Hayes, S.; Zhang, W.; Branthwaite, M.; Jones, F. Self-Healing of Damage in Fibre-Reinforced Polymer-Matrix Composites. *J. R. Soc., Interface* **2007**, *4*, 381−387.
(30) Brown, E. N.; Sottos, N. R.; White, S. R. Fracture Testing of a Self-Healing Polymer Composite. *Exp. Mech.* **2002**, *42*, 372−379.
(31) Brown, E. N.; White, S. R.; Sottos, N. R. Retardation and Repair of Fatigue Cracks in a Microcapsule Toughened Epoxy Composite—Part II: In Situ Self-Healing. *Compos. Sci. Technol.* **2005**, *65*, 2474−2480.
(32) Brown, E. N.; White, S. R.; Sottos, N. R. Retardation and Repair of Fatigue Cracks in a Microcapsule Toughened Epoxy Composite—Part I: Manual Infiltration. *Compos. Sci. Technol.* **2005**, *65*, 2466−2473.
(33) Laubengayer, A. W.; Finlay, G. R. Donor-Acceptor Bonding. I. Etherates of Boron Trifluoride. *J. Am. Chem. Soc.* **1943**, *65*, 884−889.
(34) Wool, R.; O'Connor, K. A Theory of Crack Healing in Polymers. *J. Appl. Phys.* **1981**, *52*, 5953−5963.
(35) Yuan, Y. C.; Rong, M. Z.; Zhang, M. Q.; Yang, G. C.; Zhao, J. Q. Healing of Fatigue Crack in Epoxy Materials with Epoxy/Mercaptan System via Manual Infiltration. *eXPRESS Polym. Lett.* **2010**, *4*, 644−658.
(36) Yuan, Y. C.; Rong, M. Z.; Zhang, M. Q.; Yang, G. C.; Zhao, J. Q. Self-Healing of Fatigue Crack in Epoxy Materials with Eepoxy/Mercaptan System. *eXPRESS Polym. Lett.* **2011**, *5*, 47−59.
(37) Wolf, E. Fatigue Crack Closure under Cyclic Tension. *Eng. Fract. Mech.* **1970**, *2*, 37−45.